

BEACON: A Bayesian Optimization Inspired Strategy for Efficient Novelty Search

Wei-Ting Tang¹, Ankush Chakrabarty² *Senior Member, IEEE*, and Joel A. Paulson^{1,*} *Senior Member, IEEE*

Abstract—Novelty search (NS) refers to a class of exploration algorithms that automatically uncover diverse system behaviors through simulations or experiments. Uncovering diversity is a key aspect of engineering design problems with connections to material and drug discovery, neural architecture search, reinforcement learning, and robot navigation. Since the relationship between the inputs and behaviors (outputs) of modern engineering systems not always available or easily represented in closed analytical form, novelty search must be able to handle model opacity. For systems whose behaviors are expensive to simulate or evaluate, we propose a sample-efficient NS method inspired by Bayesian optimization principles. This involves modeling the input-to-behavior mapping with multi-output Gaussian processes (MOGP) and selecting inputs to evaluate that maximize a novelty metric while balancing the exploration-exploitation trade-off. By leveraging advances in efficient posterior sampling and high-dimensional Gaussian process modeling, we discuss how our approach can be made scalable with respect to both the amount of data and number of inputs. We demonstrate the potential of our approach on several well-studied benchmark problems and multiple real-world examples. We show that BEACON comprehensively outperforms existing baselines by finding substantially larger sets of diverse behaviors under limited sampling budgets.

Index Terms—Gaussian processes; Bayesian active learning; Novelty search; Sample-efficient discovery

I. INTRODUCTION

With the increased modeling complexity of modern engineering systems, it is often easier to represent the system input-output behavior via black-box functions f whose arguments are user-defined system inputs $x \in \mathcal{X}$ that yield outcomes (or behaviors) via the map $f : \mathcal{X} \mapsto \mathcal{O}$ in some outcome space \mathcal{O} ; we will define notation more rigorously later. Derivative-free search methods ranging from simplices (e.g., Nelder-Mead), meta-heuristic population-based algorithms (e.g. particle swarms), and surrogate-based optimization (e.g. Bayesian optimization) provide powerful tools to *optimize* the quality of the outcomes based on a pre-defined criteria of optimality; c.f. [1]–[4] of an overview of these classes of algorithms. If instead of seeking the highest quality outcomes we are interested in understanding the range of outcomes that can be rendered possible by the black-box system, then a different approach is required.

Let us consider the following motivating example. Suppose f denotes the solution map of a forced Duffing oscillator and

¹WTT and JAP are affiliated with the Department of Chemical and Biomolecular Engineering, The Ohio State University, Columbus, OH, USA.

²AC is affiliated with Mitsubishi Electric Research Laboratories, Cambridge, MA, USA.

*Corresponding author. Email: paulson.82@osu.edu

x are the parameters of the oscillator and the external forcing function. We know that the solutions of the Duffing oscillator are either chaotic, periodic, quasi-periodic, or asymptotically convergent to a fixed point depending on the values of x [5]. If our objective was to numerically discover the range of behaviors of f with no prior knowledge of the fact that these behaviors are possible, we would struggle to put it into an optimization framework. First, because there is no clear objective function that will induce all of these behaviors simultaneously, e.g. minimizing or maximizing Lyapunov exponents will only yield convergence to a fixed point or chaotic oscillations, but not the intermediate periodic behaviors. Second, such an objective landscape would be fraught with local optima, and extremely hard to navigate without exorbitant function evaluations. A more natural solution to uncovering diverse behaviors is possible by novelty search, wherein the focus is shifted to pure exploration.

Instead of optimizing a pre-defined objective, novelty search aims to discover a new behavior of f given all past observed behaviors by modifying x and defining (actually, optimizing) a ‘novelty metric’ [6], [7]. This is especially useful for automated scientific discovery such as for learning new protocell behaviors [8], novel material design [9], and scenario generation to inform policy search in reinforcement learning [10]. The NS perspective has also been found to be very useful in so-called ‘deceptive problems’ wherein the optimization path taken towards a specific objective can often get stuck in suboptimal solutions. Since the mapping between inputs and system outcomes is generally unknown, established NS methods rely on meta-heuristics, such as evolutionary algorithms, to select new evaluation points. Genetic Algorithms (GAs) have frequently been employed in this context. For instance, the authors of [11] proposed diversity-promoting mechanisms to address deceptive optimization landscapes. Similarly, swarm intelligence techniques such as Particle Swarm Optimization (PSO) have been adapted for novelty search, as demonstrated by [12], who explored behavioral diversity for robotics applications. Furthermore, the MAP-Elites algorithm introduced by [13] integrates population-based exploration to balance diversity and performance metrics. However, these methods are known to be *sample-inefficient*, requiring a very large number of evaluations, which limits their use on expensive-to-evaluate systems.

We take inspiration from the fundamental principles of Bayesian optimization (BO) to propose a Bayesian novelty search algorithm that exhibits high sample-efficiency. To this end, we construct Gaussian process (GP) surrogate models [14] to learn the unknown system’s input-output mapping. Unlike

BO, our surrogate models do not approximate optimization objectives but instead represent outcomes that a user wishes to explore. The outcome space can be freely defined by the user, meaning it can be a multi-element vector encompassing all the user's desired features of exploration. For example, in drug discovery, this vector could comprise the efficacy, size, synthesizability, and stability of a candidate drug compound.

Our *main contributions* are summarized as follows: (i) We introduce a new NS algorithm, referred to as **BEACON** (**B**ayesian **E**xploration **A**lgorithm for **o**ut**C**o**M**e Novelty), for noisy, expensive black-box systems that is designed to discover unseen behaviors of the system using a minimal number of evaluations; (ii) we propose a novel Thompson sampling-based acquisition function for NS applications that, to our knowledge, is the first to address the exploration-exploitation trade-off, handle stochastic observations noise, and is suitable for gradient-based acquisition function optimization; (iii) we improve the scalability of the core BEACON algorithm to high-dimensional problems including a general approach that uses fully Bayesian sparsity-inducing function priors and a specialized approach for computational chemistry applications; and (iv) we conduct extensive experiments on several synthetic and real-world problems that demonstrate the substantial benefits BEACON can achieve in terms of identified behaviors over relevant existing NS works. These include a first-time application of NS to discovery of metal organic frameworks that are useful materials in clean energy applications, and a challenging molecular discovery benchmark problems with 2133 input dimensions.

The rest of the paper is organized as follows. In Section II, we present some necessary background, introducing BO terminology, multi-output GP regression, and NS basics. Notation is also fixed in this section. In Section III, we present the proposed BEACON algorithm, along with pseudocode. We also provide additional customization for high-dimensional problems, and for problems where domain-relevant behavior constraints exist. Our validation of BEACON and baseline comparisons on benchmark problems is presented in Section IV, along with multiple real-world applications that reflect the potential of the base BEACON algorithm, along with the potency of the customization provided for scalability and constraint-handling, both on CPU and GPU.

II. PRELIMINARIES

A. Novelty Search

In novelty search, the goal is to encourage exploration by rewarding inputs that exhibit unique behaviors compared against previously evaluated inputs. We consider the behavior of a system to be characterized by a vector-valued black-box function $\mathbf{f} : \mathcal{X} \rightarrow \mathcal{O}$ with $\mathbf{f} = (f^{(1)}, \dots, f^{(n)})$ that maps an admissible input space $\mathcal{X} \subset \mathbb{R}^d$ to a possibly multi-output outcome space $\mathcal{O} \subset \mathbb{R}^n$ that are both compact. We assume that neighboring values in outcome space share similar behaviors. To express this mathematically, we define a discrete (finite) behavior space \mathcal{B} that is an ϵ -cover of \mathcal{O} , i.e., for some $\epsilon > 0$, $\forall \mathbf{y} \in \mathcal{O}, \exists \mathbf{y}' \in \mathcal{B}$ such that $\|\mathbf{y} - \mathbf{y}'\| \leq \epsilon$.

Now suppose we define a distance metric $\rho : \mathcal{O} \times \mathcal{O} \rightarrow \mathbb{R}_{\geq 0}$ on pairs of outcomes. Then a novelty score ζ is defined

by $\zeta(\mathbf{x}) = \rho(\mathbf{f}(\mathbf{x}), \mathcal{O}')$, where $\mathcal{O}' \subseteq \mathcal{O}$ is an archive of previously observed outcomes against which novelty of \mathbf{x} is being measured. In general, we formulate a novelty score as

$$\zeta(\mathbf{x}) = \mathbf{A}(\{\rho(\mathbf{f}(\mathbf{x}), \mathbf{o}') \mid \mathbf{o}' \in \mathcal{O}'\}), \quad (1)$$

where $\mathbf{A} : 2^{\mathbb{R}_{\geq 0}} \rightarrow \mathbb{R}_{\geq 0}$ is an accumulation operator such as the mean or maximum, and the argument of \mathbf{A} represents the set of distances from $\mathbf{f}(\mathbf{x})$ to each behavior in the archive \mathcal{O}' .

An example of ζ using the k -nearest neighbors metric is

$$\zeta_{k\text{NN}}(\mathbf{x}) = \frac{1}{k} \sum_{i=1}^k \|\mathbf{f}(\mathbf{x}) - \mathbf{f}(\mathbf{x}_i)\|. \quad (2)$$

Here, the accumulator \mathbf{A} would be the expectation operation, ρ the Euclidean distance defined on \mathcal{O} , and $\{\mathbf{x}_i\}_{i=1}^k$ denote the k -nearest neighbors to \mathbf{x} with respect to values they induce in the outcome space through \mathbf{f} .

Population-based NS algorithms has shown to be effective at discovering diverse function behavior by keeping populations with high k -nearest novelty score and perform mutations to generate possibly novel function behavior. However, these algorithms typically require large population sizes, and therefore, an exorbitant number of function evaluations (NFEs), which is not favorable for the case that function evaluation is expensive. In comparison, BO is known to have high sample efficiency in black-box settings. A brief description of BO is provided next.

B. Bayesian Optimization

BO is a sequential decision-making strategy to efficiently find a global optimum $\mathbf{x}^* = \operatorname{argmin}_{\mathbf{x} \in \mathcal{X}} f(\mathbf{x})$ for an expensive-to-evaluate black-box function f , where \mathcal{X} represents the admissible search space. Classical BO performs the following two steps *ad infinitum*, or until a predefined sampling budget is exhausted: (1) Constructing uncertainty-aware (probabilistic) surrogate models based on previously sampled data pairs $\{(\mathbf{x}, y)\}$ where y is a possibly noisy observation of $f(\mathbf{x})$ and (2) Optimizing an acquisition function (AF) that provides some measure of how valuable a future point is to sample by balancing the exploration-exploitation trade-off during the BO search process. Common acquisition functions include upper confidence bound (UCB) [15], expected improvement (EI) [16], and Thompson sampling (TS) [17]. TS is a randomized approach for sequential decision making under uncertainty and has been shown to provide strong empirical performance in BO [18]. TS works by selecting $\operatorname{argmin}_{\mathbf{x} \in \mathcal{X}} g(\mathbf{x})$ as the next sample location where g is a posterior realization of the probabilistic surrogate model.

Gaussian process (GP) models [14] are the most common choice of surrogate model in BO. The underlying assumption in GPs is that the outputs at any finite collection of inputs can be modeled by a multivariate Gaussian distribution. This implies that a GP prior is fully specified by a prior mean function $\mu(\mathbf{x})$ and a prior kernel function $\kappa(\mathbf{x}, \mathbf{x}')$ that specifies the covariance of any two function values $f(\mathbf{x})$ and $f(\mathbf{x}')$ for any $\mathbf{x}, \mathbf{x}' \in \mathcal{X}$. The kernel encodes key information related to the underlying properties of the function (such as smoothness and stationarity) and so is problem-dependent. The

methods we discuss in this work can be generally applied to any valid kernel function, though one should only expect good performance in cases where the kernel is well-aligned to the problem at hand. Since we typically do not know the optimal kernel *a priori*, one usually introduces hyperparameters in the kernel that can be tuned given available data (further details on this point are provided in Section IV).

Given a GP prior, we can infer (predict) the function value $f(\mathbf{x})$ at an arbitrary test point $\mathbf{x} \in \mathcal{X}$ given a set of N function observations denoted by $\mathcal{A} = \{(\mathbf{x}_i, y_i)\}_{i=1}^N$ where $y_i = f(\mathbf{x}) + \eta_i$ and $\eta_i \in \mathcal{N}(0, \sigma^2)$ is a noise term with mean zero and variance σ^2 . Conditioned on \mathcal{A} , the posterior remains a GP with the following mean and kernel functions

$$\begin{aligned}\mu_{\mathcal{A}}(\mathbf{x}) &= \mu(\mathbf{x}) + \kappa_{\mathcal{A}}^{\top}(\mathbf{x})\tilde{\mathbf{K}}_{\mathcal{A}}^{-1}(\mathbf{y} - \mu_{\mathcal{A}}), \\ \kappa_{\mathcal{A}}(\mathbf{x}, \mathbf{x}') &= \kappa(\mathbf{x}, \mathbf{x}') - \kappa_{\mathcal{A}}^{\top}(\mathbf{x})\tilde{\mathbf{K}}_{\mathcal{A}}^{-1}\kappa_{\mathcal{A}}(\mathbf{x}'),\end{aligned}\quad (3)$$

where $\mathbf{y} = [y_1, \dots, y_N]^{\top}$, $\mu_{\mathcal{A}} = [\mu(x_1), \dots, \mu(x_N)]^{\top}$, $\kappa_{\mathcal{A}}(\mathbf{x}) \in \mathbb{R}^N$ is the vector of covariance values between the test input \mathbf{x} and the observed inputs in \mathcal{A} , and $\tilde{\mathbf{K}}_{\mathcal{A}} = \mathbf{K}_{\mathcal{A}} + \sigma^2 \mathbf{I}_N$ with $\mathbf{K}_{\mathcal{A}} \in \mathbb{R}^{N \times N}$ denoting the covariance matrix between all observed inputs in \mathcal{A} .

III. PROPOSED BAYESIAN EXPLORATION FOR OUTCOME NOVELTY SEARCH

Recall that \mathcal{O} is the outcome space, and \mathcal{B} is the discrete set of unique behaviors whose cardinality (or a lower bound) $|\mathcal{B}|$ is known. Suppose $\varphi : \mathcal{O} \mapsto \mathcal{B}$ be the function that maps an outcome of the system to a specific behavior. In Bayesian novelty search, we are interested in identifying inputs that cover as much of the behavior space \mathcal{B} as possible. Since each evaluation of f is expensive, we want to uncover a diverse range of behaviors over a finite and discrete sample budget $\{\mathbf{x}_t\}_{t=1}^T$. We can also handle the case when the function f is noisy, and therefore a measurement of the outcome function yields $\mathbf{y}_t = f(\mathbf{x}_t) + \eta_t$. We assume that the noise $\eta_t \sim \mathcal{N}(0, \sigma^2 \mathbf{I}_n)$ is isotropic Gaussian with zero-mean and standard deviation $\sigma \in \mathbb{R}_+$.

In order to ascertain our coverage of the behavior space \mathcal{B} , we define a behavior gap at iteration t by the quantity:

$$\text{BG}_t = 1 - (|\{\varphi(f(\mathbf{x}_1)), \dots, \varphi(f(\mathbf{x}_t))\}| / |\mathcal{B}|).$$

This allows us to measure the fraction of unobserved behaviors in the system. Our *objective* is to minimize the cumulative behavior gap $\sum_{t=1}^T \text{BG}_t$, or equivalently, maximize the fraction of unique behaviors observed thus far.

Since f is unknown, we cannot directly minimize the cumulative behavior gap. Instead, we adopt an intelligent sequential learning strategy inspired by BO. In the general case where f is a multi-output function, a multi-output surrogate modeling approach is necessary. To this end, we model f using a multi-output Gaussian process (MOGP) prior, which is particularly well-suited for problems where f exhibits smoothness properties, such as membership in a reproducing kernel Hilbert space (RKHS) [19]. The MOGP enables the construction of a posterior distribution $\mathbb{P}(f|\mathcal{D}_t)$ over the true function f , given observed data $\mathcal{D}_t = \{(\mathbf{x}_i, y_i)\}_{i=1}^t$. Critically, the posterior mean and covariance function in the multi-output setting

can still be computed analytically. By extending the kernel definition to incorporate the output index as an additional input, i.e., $\kappa((\mathbf{x}, j), (\mathbf{x}', j'))$, the standard posterior predictive equations for single-output Gaussian processes in (3) remain applicable. In cases where the outputs are independent, the kernel simplifies to a block-diagonal structure, and the MOGP reduces to independent GP regressions for each output.

Although general novelty scores ζ can be proposed as in (1), we restrict our initial discussion (for simplicity) to the novelty score based on nearest neighbors, ζ_{KNN} , presented in (2). Evaluating ζ_{KNN} requires access to the true function f , which is unavailable since f is a black-box function. Furthermore, we must account for the uncertainty in evaluating f , as the observed values $\varphi(\mathbf{y})$ may differ from the true values $\varphi(f(\mathbf{x}))$ due to noise η . This discrepancy can lead to inaccuracies in the distance metric ρ , causing it to select spurious neighbors thus making the novelty score sensitive to noise. We can use the MOGP surrogate to help overcome these challenges. Given a dataset \mathcal{D} , we denote the MOGP posterior by $\text{MOGP}(\mu_{\mathcal{D}}, \kappa_{\mathcal{D}})$, where $\mu_{\mathcal{D}}(\mathbf{x})$ is the vector-valued mean function and $\kappa_{\mathcal{D}}(\mathbf{x}, \mathbf{x}')$ is a matrix-valued covariance function with elements. The MOGP serves two key purposes: (i) it filters observation noise by replacing noisy data with surrogate predictions, and (ii) it enables uncertainty-aware decision-making by allowing us to "fantasize" potential realizations of f , for instance, through Thompson sampling [17], which can be performed efficiently; see [20].

To incorporate these capabilities into the algorithm, we draw a Thompson sample $\hat{f}(\mathbf{x}) \sim \text{MOGP}(\mu_{\mathcal{D}_t}, \kappa_{\mathcal{D}_t})$ from the MOGP posterior conditioned on the data \mathcal{D}_t collected up to the t -th iteration. Using this sample, we define the following acquisition function (to be maximized):

$$\alpha_{\text{NS}}(\mathbf{x} | \hat{f}, \mathcal{D}_t) := \frac{1}{k} \sum_{i=1}^k \rho(\hat{f}(\mathbf{x}), \mu_{\mathcal{D}_t}(\mathbf{x}_i^*)), \quad (4)$$

which serves as a computationally tractable proxy for the novelty score (2). For a given \mathbf{x} , the points $\{\mathbf{x}_i^*\} \subset \{\mathbf{x}_1, \dots, \mathbf{x}_N\}$ are the k nearest neighbors to $\hat{f}(\mathbf{x})$, based on the posterior mean predictions $\{\mu_{\mathcal{D}_t}(\mathbf{x}_1), \dots, \mu_{\mathcal{D}_t}(\mathbf{x}_N)\}$ of the MOGP. Closeness is measured using the same distance metric ρ as in (2). By maximizing $\alpha_{\text{NS}}(\mathbf{x})$ over the input domain \mathcal{X} , we identify an \mathbf{x}_{t+1} such that the distance from $\hat{f}(\mathbf{x}_{t+1})$ to its k nearest neighbors is maximized. This encourages exploration by promoting the discovery of novel behaviors and unseen outcomes. Once \mathbf{x}_{t+1} is selected, we evaluate $f(\mathbf{x}_{t+1})$ to obtain \mathbf{y}_{t+1} , update the dataset $\mathcal{D}_{t+1} = \mathcal{D}_t \cup \{(\mathbf{x}_{t+1}, \mathbf{y}_{t+1})\}$, and repeat the BEACON loop.

To maximize the acquisition function efficiently, we would like to take advantage of gradient-based methods with fast convergence and low memory complexity, such as L-BFGS-B [21]. This is possible by recasting (4) in terms of the sort operator:

$$\alpha_{\text{NS}}^{\text{sort}}(\mathbf{x}) = \frac{1}{k} \mathbf{e}_k^{\top} \text{sort} \left[\rho(\hat{f}(\mathbf{x}), \mu_{\mathcal{D}}(\mathbf{x}_q)) \right]_{q=1:N} \quad (5)$$

where \mathbf{e}_k is a vector whose first k entries are equal to 1 and the remaining entries are equal to 0 and sort denotes an operator that sorts the column vector argument in descending order. As

discussed in [22], the standard sort operator is continuous and almost everywhere differentiable (with non-zero gradients).

Algorithm 1 presents the overall pseudocode for the BEACON approach. In order to provide intuition as to BEACON’s behavior, we show some insightful BEACON iterations in Figure 1. The left, middle, and right columns correspond to BEACON iterations 1, 5, and 9 (the final iteration), respectively. The top row shows the true function (black line), the evolution of the surrogate model (mean with blue dotted line and confidence interval as blue shaded region), and a single Thompson sample (green dotted line). At each iteration, BEACON selects the new query point (depicted by a red star) that maximizes our proposed acquisition function α_{NS} . In the lower row of plots, we depict the discretization levels used to define different system behaviors with rectangular bands: unfilled white bands indicate those behaviors have not yet been discovered, and colored bands indicate BEACON has discovered that behavior; there are 10 behaviors, therefore 10 bands. As the algorithm progresses, we see BEACON consistently finds new behaviors through effective exploration of the outcome space. At the first iteration, 4 out of 10 behaviors has been discovered by the sampling points, resulting in $\text{BG}_t = 60\%$. At iteration 9, BEACON can reach $\text{BG}_t = 0\%$, indicating that all possible behaviors has been discovered and the algorithm has converged.

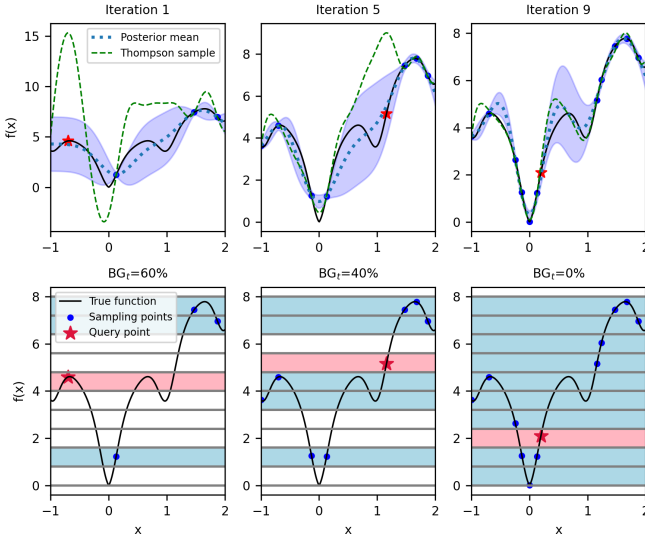


Fig. 1. Visual illustration of the fully sequential version of BEACON applied to the 1-D Ackley function.

Remark 1. *The compute required to sort in (5) can become significant for large N . To counteract this, we suggest only keeping track of outcomes that lead to unique behaviors and then calculating the k -nearest neighbors to just those outcomes. By doing so, we limit the sorting complexity to $\mathcal{O}(|\mathcal{B}| \log |\mathcal{B}|) \ll \mathcal{O}(N \log N)$.*

Remark 2. *We present an asynchronous form of BEACON in Algorithm 1 that takes advantage of $M \geq 1$ parallel workers motivated by problems that can exhibit asynchronism; e.g., in*

Algorithm 1 BEACON Pseudocode

```

1: Input: Outcome function  $f$ , input domain  $\mathcal{X}$ , initial data  $\mathcal{D}$ , budget  $T$ , number of nearest neighbors  $k$ , outcome distance metric  $\rho(\cdot)$ , MOGP prior  $\text{MOGP}(\mu, \kappa)$ .
2: Initialize: Data  $\mathcal{D}_0 \leftarrow \mathcal{D}$  and surrogate model  $\text{MOGP}_0 \leftarrow \text{MOGP}(\mu_{\mathcal{D}_0}, \kappa_{\mathcal{D}_0})$ .
3: for  $t = 1, 2, \dots, T$  do
4:   if  $t > M$  then
5:      $\mathbf{x}' \leftarrow$  previous query point
6:      $\mathbf{y}' = f(\mathbf{x}') + \eta \leftarrow$  function evaluation
7:     Update dataset  $\mathcal{D}_t \leftarrow \mathcal{D}_{t-1} \cup \{(\mathbf{x}', \mathbf{y}')\}$ 
8:     Retrain surrogate  $\text{MOGP}_t \leftarrow \text{MOGP}(\mu_{\mathcal{D}_t}, \kappa_{\mathcal{D}_t})$ .
9:   else
10:     $\mathcal{D}_t \leftarrow \mathcal{D}_{t-1}$  and  $\text{MOGP}_t \leftarrow \text{MOGP}_{t-1}$ .
11:   end if
12:    $\hat{\mathbf{f}} \leftarrow$  Thompson sample from  $\text{MOGP}_t$ 
13:    $\mathbf{x}_t \leftarrow \arg \max_{\mathbf{x} \in \mathcal{X}} \alpha_{\text{NS}}(\mathbf{x} | \hat{\mathbf{f}}, \mathcal{D}_t)$ 
14:   Deploy worker to evaluate  $f(\mathbf{x}_t)$ 
15: end for

```

material discovery. Once a worker finishes a job, it becomes available to begin a new evaluation.

Remark 3. *As we will show in the various case studies in Section V, the core BEACON algorithm can easily be extended to handle a wide range of problems. This is because there are a few components of BEACON that are customizable to the specific problem: in particular, we show how to handle high-dimensional input spaces by appropriate kernel selection, along with how to incorporate user-feedback and prior information on behaviors.*

IV. PERFORMANCE COMPARISON AND ABLATIONS

In this section, we compare BEACON against established NS methods for the purposes of benchmarking performance on well-studied synthetic functions. The section begins by discussion the implementation details for BEACON, the synthetic functions, and the competitor algorithms, before demonstrating that BEACON can outperform all competitors comprehensively on these test problems. We also provide empirical evidence based on ablation studies that the algorithm is quite robust to design choices.

A. BEACON Implementation

All implementations of Gaussian processes and its variants were performed using GPyTorch [23] and BoTorch [24] in Python 3.11 in a Ubuntu operating system running an Intel(R) Core(TM) i7-10700K 3.8 GHz CPU.

All MOGPs in our experiments have a covariance function $\kappa((\mathbf{x}, j), (\mathbf{x}', j')) = \delta_{jj'} \kappa_j(\mathbf{x}, \mathbf{x}')$ where $\delta_{jj'}$ is the Kronecker delta, which implies all outputs are modeled independently. For the synthetic experiments, the GPs have a constant mean function and a covariance radial basis function (RBF) with automatic relevance determination. We estimate the GP hyperparameters (and noise variance σ^2) using maximum likelihood estimation using standard settings of the

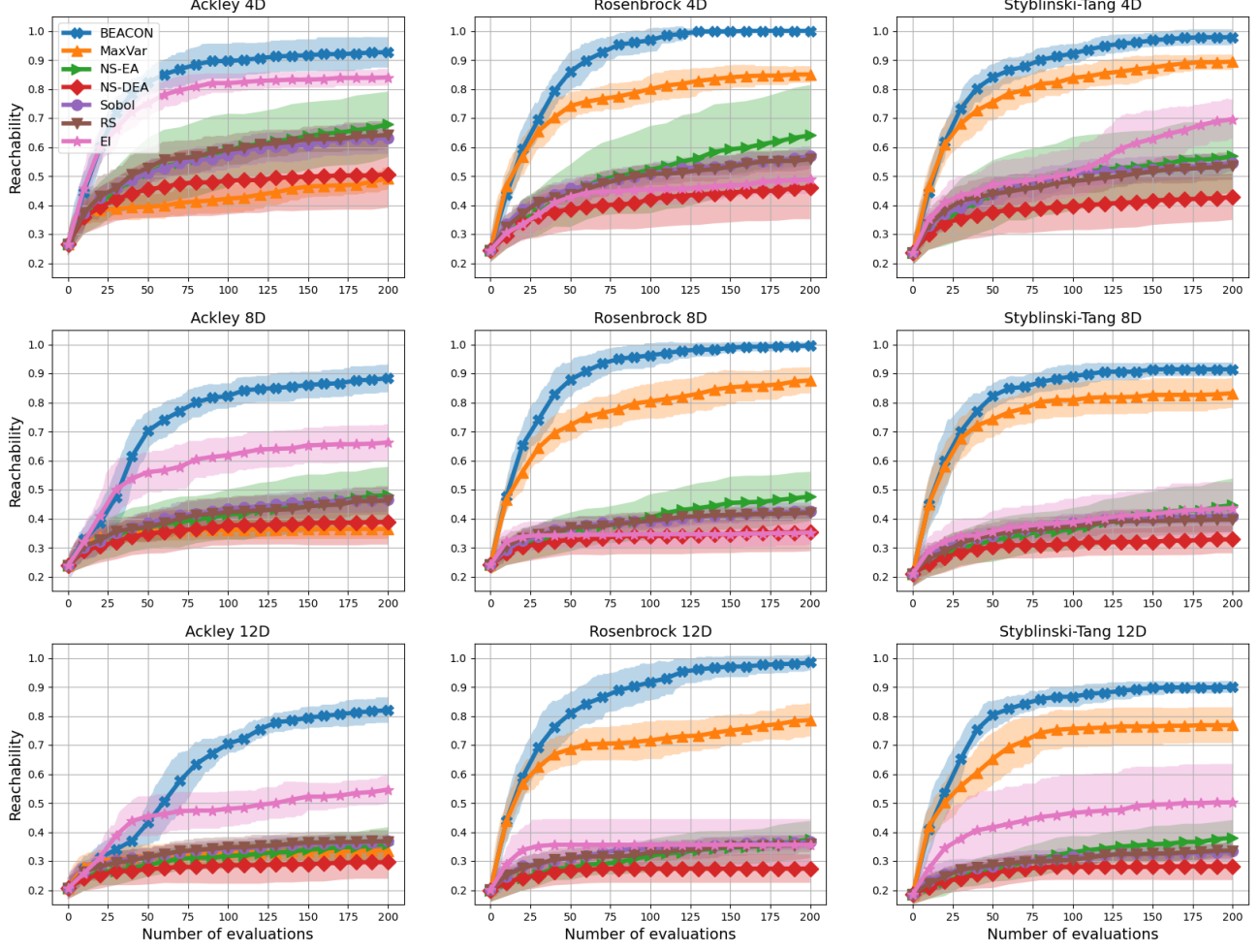


Fig. 2. Results on synthetic test problems for Ackley, Rosenbrock, and Styblinski-Tang with 4, 8, and 12 dimensions. BEACON provides substantially better outcome reachability over the benchmark methods, with larger improvements for higher-dimensional problems.

`fit_gpytorch_mll` function. We use the efficient Thompson sampling (TS) method proposed in [20] that yields a high-accuracy continuously differentiable realization \hat{f} . We then develop a PyTorch-based implementation of α_{NS} in 5 that we maximize using the SciPy implementation of L-BFGS-B [21] over a random set of multi-start initial conditions, as done in BoTorch’s `optimize_acqf` function.

B. Synthetic Functions and Competitor Algorithms

1) *Single-Outcome Functions*: We set up synthetic test functions based on the following benchmark functions [25], all in D -dimensions: the Ackley function, the Rosenbrock valley function, and the Styblinski-Tang function, given by

$$\begin{aligned} f_{\text{ackley}}(\mathbf{x}) &= -20e^{-\|\mathbf{x}\|/5} - e^{\frac{1}{D} \sum_{i=1}^D \cos(2\pi x_i)} - 17.2817, \\ f_{\text{rosen}}(\mathbf{x}) &= \sum_{i=1}^{D-1} [100(x_{i+1} - x_i^2)^2 + (1 - x_i)^2], \\ f_{\text{stybtang}}(\mathbf{x}) &= \frac{1}{2} \sum_{i=1}^D (x_i^4 - 16x_i^2 + 5x_i), \end{aligned}$$

respectively. We test BEACON for the cases $D = 4, 8, 12$ on 100 runs. We treat the output of these functions as our outcomes and partition the range of outcomes into 25 equally-spaced intervals in \mathcal{O} to define \mathcal{B} .

We also test against the following competitor NS algorithms: (i) NS-EA¹: An evolutionary algorithm for NS originally proposed in [7]. We follow the implementation of NS-EA described in [26] that starts with an initial population of size n_{pop} and then evolves each generation by randomly mutating the existing genomes. The algorithm selectively retains only the most novel genomes from the current population and the offspring, maintaining a constant population size throughout the evolutionary process. (ii) NS-DEA²: A modified version of NS-EA from [26] that replaces the novelty metric in NS-EA with a new metric ‘Distance to Explored Area’ (DEA) that measures the distance between an individual’s outcome and the convex hull of previously sampled outcomes. (iii) MaxVar: Active learning approach [15] that aims to explore regions of the sample space whose predictions are most

¹NS-EA: github.com/alaflaquierre/simple-ns.git

²NS-DEA: github.com/alaflaquierre/simple-ns.git

uncertain according to some model. (iv) Sobol: Simple quasi-random sampling algorithm [27] that is guaranteed to densely sample \mathcal{X} in the limit of infinite experimental budgets while generating well-distributed samples throughout the sampling procedure, unlike uniform random sampling. (v) RS: Uniform random sampling.

The reachability $\text{Reach}_t := 1 - \text{BG}_t$ of all algorithms across the considered problems is shown in Figure 2. It is clear that BEACON (blue) consistently outperforms the other algorithms in all cases, achieving near maximum admissible reachability of 1 in several cases and above 0.9 reachability in 15/16 cases. What is especially interesting is that other than BEACON, no single competitor algorithm performs well across the range of test cases. The CPU time taken per iteration of BEACON

TABLE I
AVG. CPU TIME PER ITERATION (MILLI-SEC) FOR TEST PROBLEMS

	ACKLEY-4D	ACKLEY-8D	ACKLEY-12D
BEACON	161	233	336
MaxVar	142	339	777
	ROSEN-4D	ROSEN-8D	ROSEN-12D
BEACON	437	703	1018
MaxVar	804	1180	1293
	STYB-TANG-4D	STYB-TANG-8D	STYB-TANG-12D
BEACON	228	540	1048
MaxVar	250	845	916

is reported in Table I, and compared against MaxVar for all the synthetic problems in this subsection. BEACON mostly requires less time compared to MaxVar: the major bottleneck for both methods is training of the GP surrogate model and optimizing the AF, but with our proposed AF and with sorting and efficient Thompson sampling, we reduce computational expenditure considerably compared to MaxVar on 7 of 9 problems. Even when MaxVar is faster the CPU times are comparable, whereas for some problems like Ackley-12D, BEACON is almost 2× more efficient in the surrogate based NS steps. We do not directly compare with the NS-EA and NS-DEA approaches because they do not have to construct surrogate models and therefore, their complexity per iteration is lower. However, they typically use many more function evaluations, which (by assumption in this work) will be much more time-consuming than any other operation.

2) *Multi-Outcome Functions*: To test BEACON in the multi-output setting, we also created a challenging *Multi-Output Plus* function with a long-tail joint distribution. This synthetic function defined over $D = 6$ inputs has two outputs, and has the form

$$\begin{aligned} y_1 &= \sin(x_1) \cos(x_2) + x_3 \exp(-x_1^2) \cos(x_1 + x_2) \\ &\quad + 0.01 \sin(x_4 + x_5 + x_6), \\ y_2 &= \sin(x_4) \cos(x_5) + x_6 \exp(-x_4^2) \cos(x_4 + x_5) \\ &\quad + 0.01 \cos(x_1 + x_2 + x_3). \end{aligned}$$

The distribution of outcomes \mathcal{O} based on 10,000 input samples drawn from the space $\mathcal{X} = [-5, 5]^D$ is shown in Figure 3. NS reachability is computed with respect to intervals defined on a 10×10 grid over the two outcomes. It is clear from the top subfigure that most of the outcomes lie near the center square around the origin. NS algorithms find such jointly long-tail

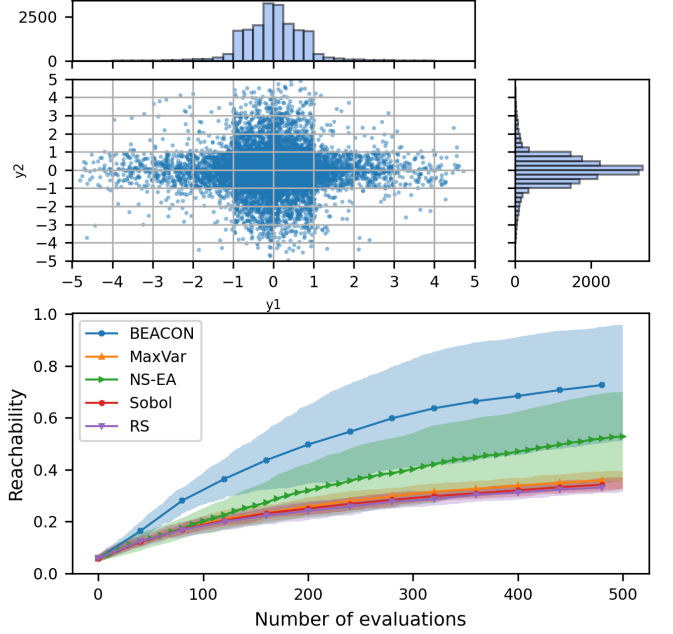


Fig. 3. (Top) Scatter plot of outcomes of multi-output cross plus function for 10,000 randomly sampled input values, with corresponding marginal histograms. (Bottom) Reachability performance results on multi-output plus function for all algorithms.

distributions challenging, as they tend to overexplore the high density center zone and ignore the tails. This is evident in the reachability results shown on the lower plot in Figure 3. In early iterations, BEACON significantly outperforms the other algorithms. Even in later iterations, BEACON discovers a larger number of behaviors despite a limited evaluation budget, finding nearly 80% while some well-known NS methods find less than 10%.

C. Ablation Studies

1) *Impact of the Resolution of Behavior Space*: In this section, we study the impact of the choice of ϵ that defines how nearby points in outcome space \mathcal{O} are divided into new behaviors \mathcal{B} . Note that we use the grid resolution as a proxy for ϵ ; that is, smaller values of ϵ correspond to fine grids. In practice, a user does not have to have an actual value for ϵ selected – as long as some “clusters” exist in the outcome space that (once observed) can be treated as behaviors, BEACON will eventually uncover them through exploration of \mathcal{O} . In other words, BEACON is designed to discover diverse outcomes that should naturally correspond to diverse behaviors as defined by a user. Therefore, ϵ only impacts how we calculate the behavior gap (and therefore, reachability). We plot the reachability performance for 2 different grid resolutions: 10 and 50 grid nodes for the 4-dimensional versions of the Ackley synthetic test problems in Figure 4. BEACON continues to be the best-performing algorithm for all grid sizes, highlighting BEACON’s robustness to the choice of \mathcal{B} .

2) *Impact of Neighborhood for Diversity Score Computation*: The choice of the number of nearest neighbors k is a hyperparameter of our algorithm. We selected it to be $k = 10$

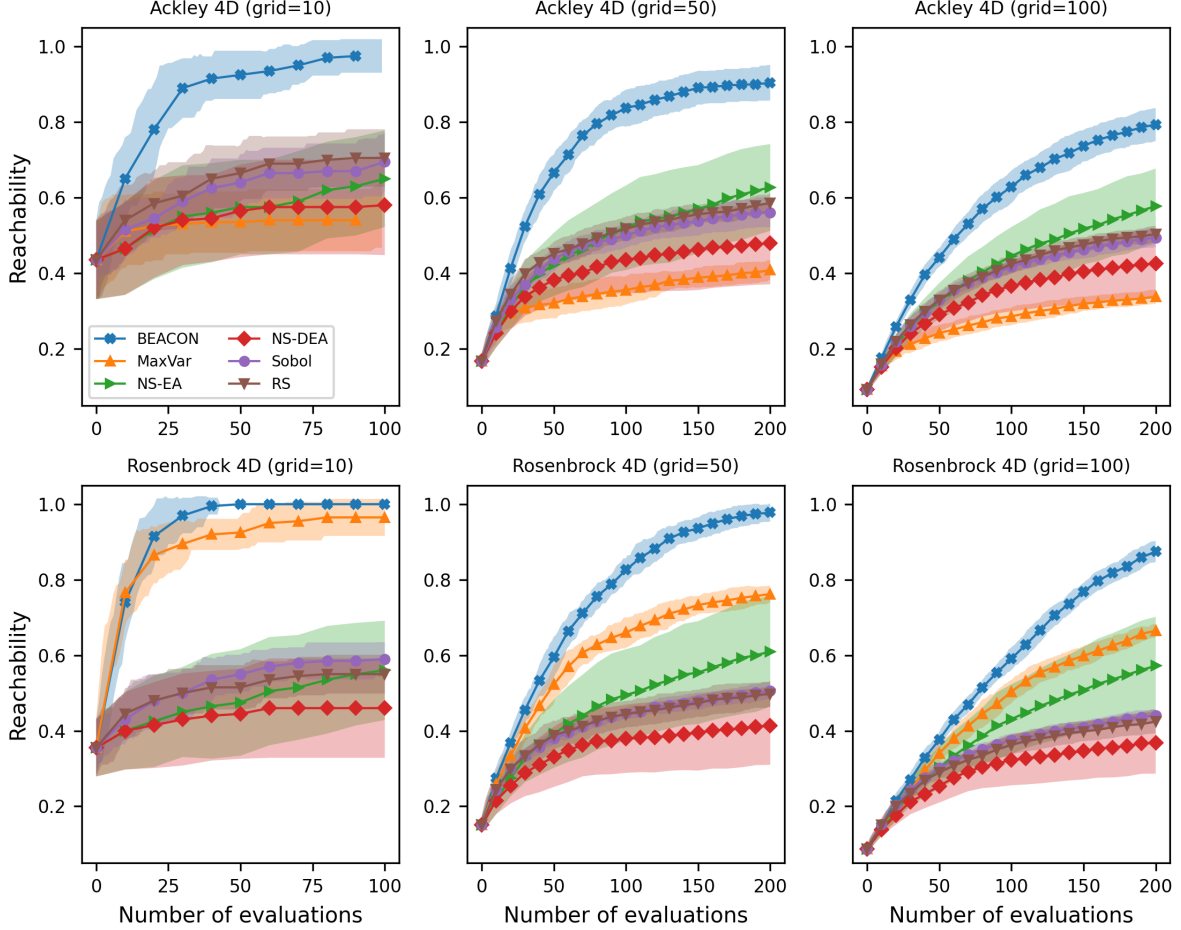


Fig. 4. Reachability performance results on (*upper row*) Ackley-4D and (*lower row*) Rosenbrock-4D for different grid resolutions.

in all case studies, as we found that to be a robust choice. We study the impact of k on the 12-dimensional versions of the synthetic test problems in Figure 5 by calculating performance for $k \in \{1, 5, 10, 20\}$. In this experiment, we use 50 initial datapoints to train the GP and use 25 equally-spaced intervals to divide outcomes into behaviors. Surprisingly, we find that even a choice of $k = 1$ does reasonably well on Rosenbrock and Styblinski-Tang, though performance does start to drop for Ackley. We see negligible difference in performance between $k = 10$ and $k = 20$, so it appears $k = 10$ is a sufficiently large value in practice.

3) *Importance of Observation Noise:* As discussed in Section III, the presence of noise in the outcome evaluation can lead to challenges in NS algorithms due to mis-categorization of behaviors, which we explore in this section. Specifically, we compare the performance of BEACON (Algorithm 1) to a noiseless variant (BEACON-noiseless) in which the acquisition function in (4) is modified by replacing $\mu_{\mathcal{D}}(\mathbf{x}_i^*)$ with y_i^* . We perform experiments on the 4d Ackley problem in which 50 initial data points are available and we divide the outcome space into 50 equally-spaced intervals to calculate reachability. Figure 6 shows the performance of BEACON and BEACON-noiseless for four different values of the noise standard deviation σ . We see BEACON outperforms BEACON-noiseless in

all cases and the gap between them widens as σ increases. This study emphasizes the importance of accounting for observation noise in NS, which, to our knowledge, has not been considered by existing NS algorithms.

V. REAL-WORLD CASE STUDIES

A. Material Discovery

Exploring materials with a diverse range of properties is critical for developing novel materials tailored to different end-use applications. Conventionally, high-throughput screening methods are employed, which rely on experiments or computer simulations to evaluate (possibly multi-property) values for a large number of randomly selected materials. While effective for large-scale exploration, these methods are computationally and experimentally expensive. BEACON offers a sample-efficient alternative by leveraging novelty search to identify under-explored regions in the material property space, significantly reducing the number of evaluations required to discover diverse materials.

For the material discovery task, we define the input space $\mathcal{X} \subset \mathbb{R}^d$ as a set of molecular descriptors that mathematically represent material candidates [28]. The outcome space $\mathcal{O} \subset \mathbb{R}^n$ corresponds to the material properties of interest (e.g.,

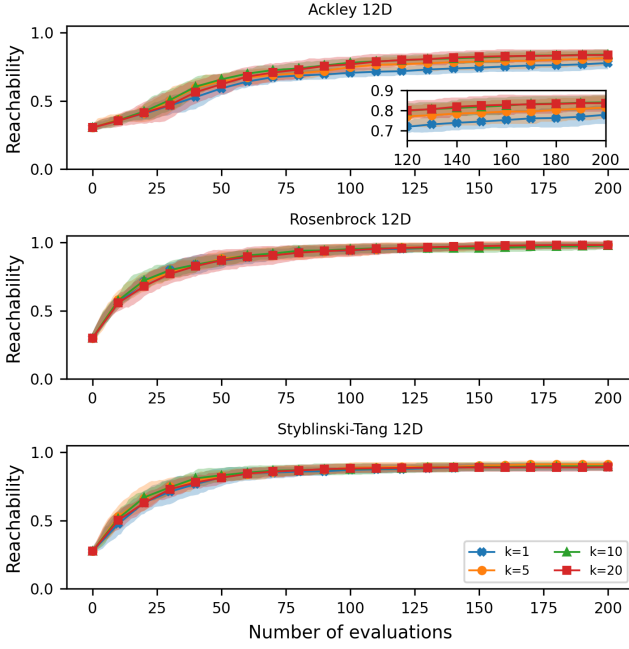


Fig. 5. Reachability performance results for BEACON on 12d Ackley (top), Rosenbrock (middle), and Styblinski-Tang (bottom) for different nearest neighbor values k .

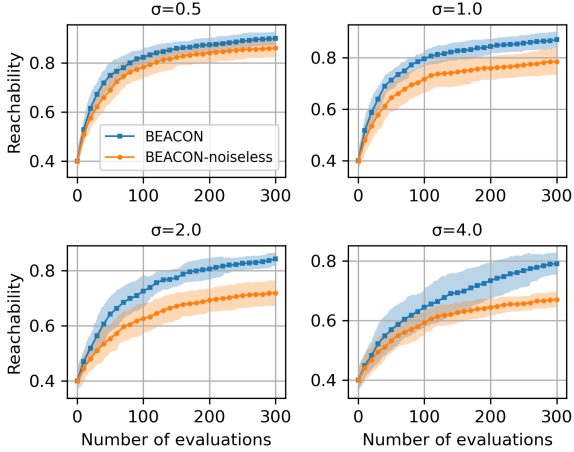


Fig. 6. Reachability performance results on 4d Ackley for BEACON (Algorithm 1) and BEACON-noiseless (variant of Algorithm 1 that treats the observations as noise-free) in the presence of noisy observations for different standard deviation noise levels.

gas uptake capacity), which may be multi-dimensional. The relationship between these spaces is modeled as a black-box function $f : \mathcal{X} \rightarrow \mathcal{O}$ that matches the problem formulation in Section II-A. Numerous methods exist to generate molecular descriptors \mathcal{X} ; the specific descriptors used in our case studies are adopted from existing literature and described in detail in the supplement.

Metal-organic frameworks (MOFs) represent an ideal testbed for this class of problems. MOFs are a diverse class of porous crystalline materials composed of metal ions and organic linkers. Their diversity arises from the effectively infinite number of possible structures that can be synthesized

by varying linkers, metal nodes, defects, and other parameters [29]. Despite their promise, there is currently no systematic framework to evaluate the chemical and property diversity of MOFs, making it difficult to identify gaps or biases in existing libraries. Recent studies [30] have demonstrated that such biases can lead to incorrect conclusions when training machine learning models for screening purposes. This highlights the need for approaches like BEACON, which efficiently explore the material property space to generate more diverse libraries of MOFs. Below, we present results for three MOF-related case studies based on experimentally determined databases (details provided in the supplement).

a) *Hydrogen uptake capacity*: Hydrogen uptake capacity is an important property in clean energy applications. We use the dataset from [31] that consists of 98,000 unique MOF structures. We develop a 7-dimensional feature representation for the input MOF. Hence, $\mathcal{X} \subset \mathbb{R}^7$, $|\mathcal{X}| = 98000$, and $\mathcal{O} \subset \mathbb{R}^1$.

b) *Nitrogen uptake capacity*: Nitrogen uptake capacity is an important property for reducing the cost of natural gas production from renewable feedstocks. We use the dataset from [32] consisting of 5,224 unique MOF structures, with a 20-dimensional feature representation for the input MOF. Hence, $\mathcal{X} \subset \mathbb{R}^{20}$, $|\mathcal{X}| = 5224$, and $\mathcal{O} \subset \mathbb{R}^1$.

c) *Joint CO_2 and CH_4 gas uptake capacity*: We also consider a multi-output MOF discovery application that treats both carbon dioxide (CO_2) uptake capacity y_1 and methane (CH_4) uptake capacity y_2 as outcomes. We use the dataset from [30] that consists of 7,000 unique MOF structures. We develop a 25-dimensional feature representation for the input MOF. Hence, $\mathcal{X} \subset \mathbb{R}^{25}$, $|\mathcal{X}| = 7000$, and $\mathcal{O} \subset \mathbb{R}^2$. The highly skewed joint outcome distribution is displayed in the supplement.

The performance of the algorithms on all MOF-related experiments is shown in Figure 7. Since the MOF problems are defined over discrete input spaces, we are unable to run NS-EA, NS-DEA, and NS-FS as they are only applicable to continuous inputs. We still observe that BEACON outperforms all other methods, achieving (on average) the highest possible reachability of 1 in all cases.

B. Drug Discovery

Exploring the chemical space to discover drug molecules with diverse properties is a critical challenge in pharmaceutical research. Property diversity is essential for identifying candidates with optimal efficacy, safety, and manufacturability, making systematic approaches to this task highly desirable. Similarly to the MOF case studies in the previous section, BEACON provides a sample-efficient alternative for navigating the vast and complex chemical space while promoting novelty in molecular properties.

For the drug discovery task, the input space $\mathcal{X} \subset \mathbb{R}^d$ represents molecular descriptors or high-dimensional feature representations of small molecules, while the outcome space $\mathcal{O} \subset \mathbb{R}^n$ corresponds to the molecular properties of interest (e.g., solubility). Although we can use the same MOGP framework for modeling the black-box property function

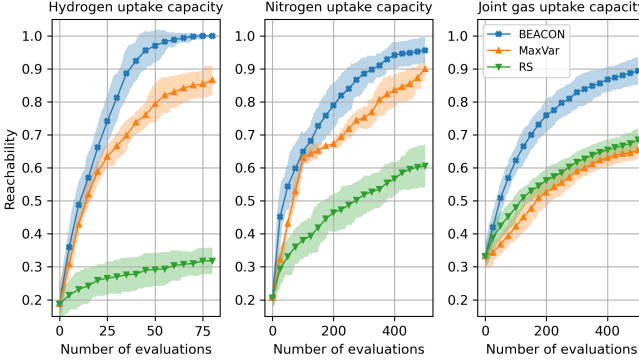


Fig. 7. Performance of BEACON and baseline methods on MOF discovery problems. Shown are results for discovering diverse MOFs with hydrogen uptake capacity (left), nitrogen uptake capacity (middle), and joint carbon dioxide and methane uptake capacities (right). The y-axis represents the reachability metric, demonstrating BEACON’s superior ability to achieve a higher range of property diversity.

$f : \mathcal{X} \rightarrow \mathcal{O}$, drug discovery problems often involve unique challenges such as high-dimensional input spaces and non-continuous molecular representations. This requires tailored modeling strategies that we discuss below.

a) *Water solubility*: We consider the dataset from [33], consisting of 900 organic compounds. We select a 14-dimensional representation of the compounds using molecular descriptors. Hence, $\mathcal{X} \subset \mathbb{R}^{14}$, $|\mathcal{X}| = 900$, and $\mathcal{O} \subset \mathbb{R}^1$.

b) *ESOL*: We evaluate BEACON on the aqueous solubility dataset containing 1,128 small organic molecules from [34]. This task uses a high-dimensional 2,133-dimensional representation based on one-hot-encoded fragprint vectors, avoiding the use of molecular descriptors. Fragprint vectors are binary representations that encode molecular features, commonly used in cheminformatics. This setup demonstrates BEACON’s ability to scale effectively to high-dimensional problems. For this task, we employ the Tanimoto-fragprint covariance function [35], which is specifically designed for non-continuous molecular inputs. Hence, $\mathcal{X} \subset \mathbb{R}^{2133}$, $|\mathcal{X}| = 1128$, and $\mathcal{O} \subset \mathbb{R}^1$.

c) *LogD*: The octanol-water partition distribution coefficient (LogD) is important in drug discovery applications as it influences several properties of drug candidates, including solubility, permeability, and toxicity. Following [36], we adopt a 125-dimensional feature representation for this dataset consisting of 2,070 molecules. Due to the high-dimensional input space, we rely on the sparse axis-aligned subspace (SAAS) prior [37], which assumes only a small number of sensitive features exist. This hierarchical prior enables BEACON to model complex high-dimensional functions while maintaining computational efficiency. Hence, $\mathcal{X} \subset \mathbb{R}^{125}$, $|\mathcal{X}| = 2070$, and $\mathcal{O} \subset \mathbb{R}^1$.

The performance of the Water Solubility, ESOL, and LogD experiments is shown in Figure 8. Again, we find that BEACON significantly outperforms all other methods in all cases, particularly in high-dimensional settings, where the SAAS prior and Tanimoto-fragprint covariance function improve BEACON’s performance.

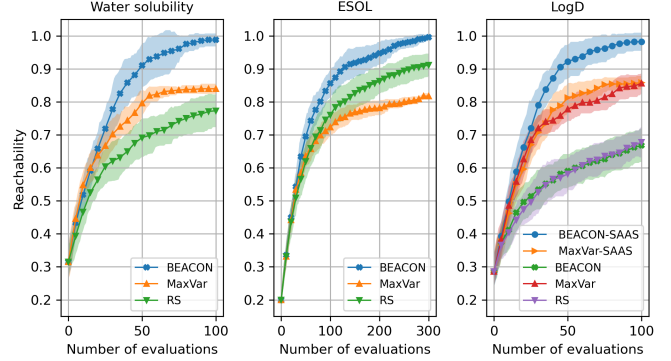


Fig. 8. Performance of BEACON and baseline methods on drug discovery problems. Shown are results for discovering small molecules with diverse properties including water solubility (left), ESOL (middle), and LogD (right). BEACON outperforms other methods across all tasks, particularly in high-dimensional settings.

C. Maze Navigation Problem

As an additional experiment, we consider a complex reinforcement learning (RL) task involving navigation through a maze. Specifically, we use the large maze configuration from the OpenAI Gymnasium [38], with further documentation available at <https://minari.farama.org/datasets/pointmaze/large/>. The objective is to guide a green ball from a specified starting location to a target location, represented by a red ball, within 300 time steps. A linear control policy is employed, which maps measured states to actions and is parameterized by eight variables that need to be optimized. The outcome space corresponds to the final landing location (x, y) of the green ball. Hence, $\mathcal{X} \subset \mathbb{R}^8$ and $\mathcal{O} \subset \mathbb{R}^2$.

This problem is particularly well-suited for novelty search (NS) due to the deceptive nature of its objective landscape: optimizing solely for the Euclidean distance between the final and target locations can result in local optima, as intermediate paths are not explicitly rewarded. To evaluate performance, we use a reward metric defined as:

$$\text{Reward} = 1 - \frac{\text{final distance to target}}{\text{initial distance to target}}.$$

This metric quantifies the improvement in proximity to the target, with an ideal reward of 1 indicating that the final location exactly matches the target.

In addition to the previously considered algorithms, we include a traditional Bayesian optimization (BO) approach using the expected improvement (EI) acquisition function [39]. In this case, the reward function is modeled with a standard GP surrogate model. This provides a direct comparison between BEACON’s NS framework and a reward-focused optimization approach.

The results for the maze navigation problem are presented in Figure 9. The top panel shows the average best observed reward across 20 replicates, where BEACON outperforms all other methods, including the objective-focused EI approach, which ranks as the second-worst performing algorithm. The bottom panel presents a violin plot of the reward distribution at the final iteration for all algorithms. BEACON is the only

method that consistently achieves successful maze navigation, with all 20 replicates yielding a final reward of 1. In contrast, other NS-based approaches, such as NS-FS and MaxVar, achieve high average rewards (at or above 0.9) in some replicates but exhibit significant variability, with several cases barely exceeding a reward of 0.5.

This case study underscores the value of BEACON's efficiency in the context of problems with deceptive objective landscapes. Notably, BEACON outperforms EI on a task explicitly designed for reward maximization. This result highlights the limitations of GP-based surrogates in modeling complex, deceptive reward functions and demonstrates BEACON's potential for broader applications involving similar challenges.

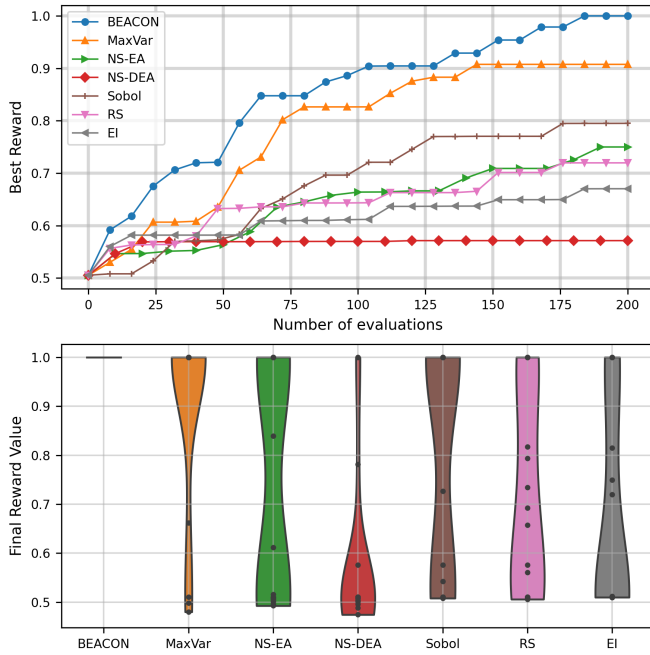


Fig. 9. Maze navigation case study. (Top) Average best observed reward for all algorithms across 20 replicates. (Bottom) Violin plot showing the distribution of best reward values at the final iteration for all algorithms.

D. Incorporating User Information and Domain Knowledge

In real-world applications, users often seek to identify specific behaviors or outcomes, incorporating prior knowledge or preferences to guide exploration. For example, a user might ask, “Can you find materials with properties in specific ranges for different applications?” [40], [41]. Such user-guided exploration can improve efficiency by focusing on regions of interest and/or avoiding redundant sampling. To address this, we extend BEACON to incorporate user information and domain knowledge, introducing the UG-BEACON (User-Guided BEACON) algorithm. UG-BEACON integrates behavior constraints by sampling only those input values x whose corresponding predicted outcomes $\hat{f}(x)$ fall outside previously observed behavior regions. This prevents redundant sampling of regions with similar behaviors, conserving the sampling budget while improving efficiency.

In this section, we evaluate UG-BEACON on two case studies: (i) discovering diverse digits in the latent space

of a generative image model with a user-defined behavior constraint and (ii) exploring an oil sorbent material design problem guided by user-defined preferences in the outcome space.

1) *Discovering Diverse Handwritten Digits from MNIST images*: Generative models, such as variational autoencoders (VAEs), allow users to generate novel outcomes by sampling from a latent space that captures essential information from high-dimensional input data. For example, VAEs have been used to explore molecular diversity by sampling from their continuous latent space [42]. Here, we apply UG-BEACON to discover diverse handwritten digits by sampling from the latent space of a VAE trained on the MNIST dataset. The behavior constraint is defined as discovering unique digits (0 through 9), with no repeated sampling of digits already classified.

We train a VAE using 10,000 MNIST images, each resized to 14x14 pixels³. The latent space is 8-dimensional, and 2,000 discrete latent variables $z \in \mathcal{Z}$ are randomly generated for exploration. UG-BEACON uses a convolutional neural network (CNN) classifier (trained to 98% validation accuracy) as a surrogate for a human evaluator. A sampled outcome is classified as a specific digit if the CNN's softmax output exceeds 0.99. As shown in Figure 10, both BEACON and UG-BEACON discover all 10 digits within the sampling budget, with UG-BEACON converging faster due to its behavior constraint, which avoids redundant sampling.

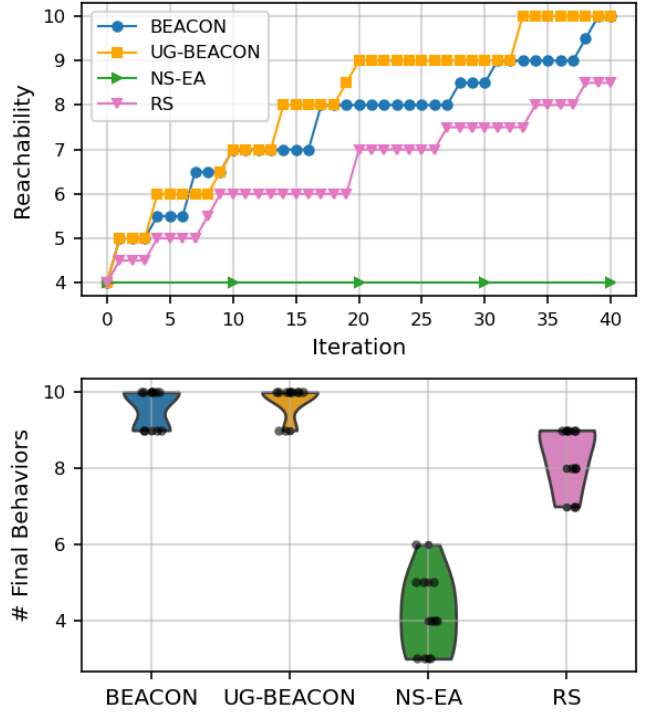


Fig. 10. MNIST case study. (Top) Average number of discovered digits for all algorithms across 10 replicates. (Bottom) Violin plot showing the distribution of discovered digits at the final iteration for all algorithms. UG-BEACON achieves faster convergence by incorporating user-defined behavior constraints on already observed digits.

³<https://github.com/williamcfrancis/Variational-Autoencoder-for-MNIST.git>

2) *Oil Sorbent Material Case Study:* Electrospun polystyrene/polyacrylonitrile (PS/PAN) materials have shown promise for oil adsorption applications. Their properties, such as water contact angle, mechanical strength, and oil adsorption capacity, can be calculated using empirical equations derived from experimental data [43]. Here, we focus on two target properties: adsorption capacity and mechanical strength. The goal is to discover as many materials as possible with diverse properties while prioritizing regions of the outcome space most relevant to practical applications.

To incorporate user preferences, we partition the 2-dimensional outcome space into four regions with different grid densities, as shown in Figure 11 (left). Regions with high mechanical strength and adsorption capacity are prioritized, reflecting their importance for practical applications. Conversely, regions with low mechanical strength and adsorption capacity are deprioritized. UG-BEACON avoids sampling in previously observed grid cells, reducing redundancy and aligning the exploration process with user-defined preferences.

For this case study, we use 10 initial samples to train the MOGP. Property values for each sample are computed using the empirical equations reported in [43]. As shown in Figure 11 (right), UG-BEACON achieves 100% reachability within 50 iterations, significantly outperforming BEACON and other state-of-the-art algorithms. BEACON struggles to reach 100% reachability, while other algorithms plateau around 90%, even after 200 iterations. These results highlight the benefits of incorporating user information into BEACON for improving efficiency and alignment with practical objectives.

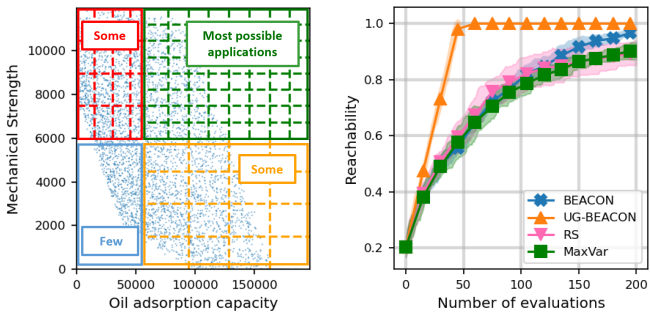


Fig. 11. Oil sorbent material case study. (Left) Partitioned 2D outcome space with user-defined behavior preferences. (Right) Reachability performance for UG-BEACON and other algorithms. UG-BEACON achieves 100% reachability within significantly fewer iterations than other methods.

VI. CONCLUSIONS AND FUTURE WORK

This paper develops an approach for efficient novelty search (NS) for systems whose outcomes are defined in terms of expensive black-box functions with noisy observations. Such problems arise in several important applications including material design, drug discovery, and reinforcement learning. Current NS methods, which are based on sample-inefficient evolutionary algorithms, struggle in the noisy low-data regime of interest in this work. Inspired by the principles of Bayesian optimization, we develop a surrogate-based NS algorithm that intelligently selects new sample locations given past

observations. We further discuss how our approach can be easily modified to scale to problems with high-dimensional input spaces and large datasets. Our extensive numerical experiments show that our proposed approach can dramatically outperform existing NS methods on synthetic and real-world problems. This includes, to our knowledge, a first time application of NS to metal organic framework discovery, which are important materials in emerging clean energy technologies.

Although we empirically observe significant benefits with our proposed approach, there are two limitations worth noting. First, it requires more computation than alternative NS methods, which we discuss in the supplement. This is not a concern for expensive systems (evaluations on the order of minutes or longer), as the improved sample efficiency more than compensates for the increased computation; however, for cheaper functions, it is not clear if our approach would still be favored. This computation gap also widens as more data is collected, though this can be controlled through appropriate choice of surrogate model (also explored in the supplement). Second, we have not established any theoretical convergence results for our method. There has been some recent work toward building a theoretical framework for NS [44], but additional work is needed to fit our approach into this framework. We believe, however, this is an exciting direction for future work.

REFERENCES

- [1] L. M. Rios and N. V. Sahinidis, “Derivative-free optimization: a review of algorithms and comparison of software implementations,” *Journal of Global Optimization*, vol. 56, no. 3, pp. 1247–1293, 2013.
- [2] B. Shahriari, K. Swersky, Z. Wang, R. P. Adams, and N. De Freitas, “Taking the human out of the loop: A review of Bayesian optimization,” *Proceedings of the IEEE*, vol. 104, no. 1, pp. 148–175, 2015.
- [3] S. J. Russell and P. Norvig, *Artificial intelligence: A modern approach*. Pearson, 2016.
- [4] P. I. Frazier, “A tutorial on Bayesian optimization,” *arXiv preprint arXiv:1807.02811*, 2018.
- [5] A. R. Zeni and J. A. Gallas, “Lyapunov exponents for a Duffing oscillator,” *Physica D: Nonlinear Phenomena*, vol. 89, no. 1-2, pp. 71–82, 1995.
- [6] J. Lehman and K. O. Stanley, “Abandoning objectives: Evolution through the search for novelty alone,” *Evolutionary Computation*, vol. 19, no. 2, pp. 189–223, 2011.
- [7] ———, “Novelty search and the problem with objectives,” *Genetic Programming Theory and Practice IX*, pp. 37–56, 2011.
- [8] J. Grizou, L. J. Points, A. Sharma, and L. Cronin, “A curious formulation robot enables the discovery of a novel protocell behavior,” *Science Advances*, vol. 6, no. 5, p. eaay4237, 2020.
- [9] K. Terayama, M. Sumita, R. Tamura, D. T. Payne, M. K. Chahal, S. Ishihara, and K. Tsuda, “Pushing property limits in materials discovery via boundless objective-free exploration,” *Chemical Science*, vol. 11, no. 23, pp. 5959–5968, 2020.
- [10] E. C. Jackson and M. Daley, “Novelty search for deep reinforcement learning policy network weights by action sequence edit metric distance,” in *Proceedings of the Genetic and Evolutionary Computation Conference Companion*, 2019, pp. 173–174.
- [11] J. Gomes, P. Mariano, and A. L. Christensen, “Devising effective novelty search algorithms: A comprehensive empirical study,” *Knowledge-Based Systems*, vol. 82, pp. 1–20, 2015.
- [12] J.-B. Mouret and S. Doncieux, “Encouraging behavioral diversity in evolutionary robotics: An empirical study,” *IEEE Transactions on Evolutionary Computation*, vol. 16, no. 1, pp. 1–15, 2012.
- [13] J.-B. Mouret and J. Clune, “Illuminating search spaces by mapping elites,” *Artificial Life*, vol. 22, no. 3, pp. 245–268, 2015.
- [14] C. K. Williams and C. E. Rasmussen, *Gaussian Processes for Machine Learning*. MIT Press Cambridge, MA, 2006, vol. 2.
- [15] N. Srinivas, A. Krause, S. M. Kakade, and M. Seeger, “Gaussian process optimization in the bandit setting: No regret and experimental design,” *arXiv preprint arXiv:0912.3995*, 2009.

[16] S. Ament, S. Daulton, D. Eriksson, M. Balandat, and E. Bakshy, “Unexpected improvements to expected improvement for bayesian optimization,” *Advances in Neural Information Processing Systems*, vol. 36, pp. 20 577–20 612, 2023.

[17] W. R. Thompson, “On the likelihood that one unknown probability exceeds another in view of the evidence of two samples,” *Biometrika*, vol. 25, no. 3-4, pp. 285–294, 1933.

[18] K. Kandasamy, A. Krishnamurthy, J. Schneider, and B. Póczos, “Parallelised Bayesian optimisation via Thompson sampling,” in *International Conference on Artificial Intelligence and Statistics*. PMLR, 2018, pp. 133–142.

[19] S. R. Chowdhury and A. Gopalan, “On kernelized multi-armed bandits,” in *International Conference on Machine Learning*. PMLR, 2017, pp. 844–853.

[20] J. Wilson, V. Borovitskiy, A. Terenin, P. Mostowsky, and M. Deisenroth, “Efficiently sampling functions from Gaussian process posteriors,” in *International Conference on Machine Learning*. PMLR, 2020, pp. 10 292–10 302.

[21] R. H. Byrd, P. Lu, J. Nocedal, and C. Zhu, “A limited memory algorithm for bound constrained optimization,” *SIAM Journal on Scientific Computing*, vol. 16, no. 5, pp. 1190–1208, 1995.

[22] S. Prillo and J. Eisenschlos, “Softsort: A continuous relaxation for the argsort operator,” in *International Conference on Machine Learning*. PMLR, 2020, pp. 7793–7802.

[23] J. Gardner, G. Pleiss, K. Q. Weinberger, D. Bindel, and A. G. Wilson, “Gpytorch: Blackbox matrix-matrix Gaussian process inference with GPU acceleration,” *Advances in Neural Information Processing Systems*, vol. 31, 2018.

[24] M. Balandat, B. Karrer, D. Jiang, S. Daulton, B. Letham, A. G. Wilson, and E. Bakshy, “BoTorch: A framework for efficient Monte-Carlo Bayesian optimization,” *Advances in Neural Information Processing Systems*, vol. 33, pp. 21 524–21 538, 2020.

[25] M. Jamil and X.-S. Yang, “A literature survey of benchmark functions for global optimisation problems,” *International Journal of Mathematical Modelling and Numerical Optimisation*, vol. 4, no. 2, pp. 150–194, 2013.

[26] S. Doncieux, G. Paolo, A. Laflaqui  re, and A. Coninx, “Novelty search makes evolvability inevitable,” in *Proceedings of the 2020 Genetic and Evolutionary Computation Conference*, 2020, pp. 85–93.

[27] I. M. Sobol’, “On the distribution of points in a cube and the approximate evaluation of integrals,” *Zhurnal Vychislitel’noi Matematiki i Matematicheskoi Fiziki*, vol. 7, no. 4, pp. 784–802, 1967.

[28] F. Sorourifar, T. Bunker, and J. A. Paulson, “Accelerating black-box molecular property optimization by adaptively learning sparse subspaces,” *arXiv preprint arXiv:2401.01398*, 2024.

[29] S. Lee, B. Kim, H. Cho, H. Lee, S. Y. Lee, E. S. Cho, and J. Kim, “Computational screening of trillions of metal-organic frameworks for high-performance methane storage,” *ACS Applied Materials & Interfaces*, vol. 13, no. 20, pp. 23 647–23 654, 2021.

[30] S. M. Moosavi, A. Nandy, K. M. Jablonka, D. Ongari, J. P. Janet, P. G. Boyd, Y. Lee, B. Smit, and H. J. Kulik, “Understanding the diversity of the metal-organic framework ecosystem,” *Nature Communications*, vol. 11, no. 1, pp. 1–10, 2020.

[31] S. Ghude and C. Chowdhury, “Exploring hydrogen storage capacity in metal-organic frameworks: A Bayesian optimization approach,” *Chemistry—A European Journal*, vol. 29, no. 69, p. e202301840, 2023.

[32] H. Daglar and S. Keskin, “Combining machine learning and molecular simulations to unlock gas separation potentials of MOF membranes and MOF/polymer MMMs,” *ACS Applied Materials & Interfaces*, vol. 14, no. 28, pp. 32 134–32 148, 2022.

[33] S. Boobier, D. R. Hose, A. J. Blacker, and B. N. Nguyen, “Machine learning with physicochemical relationships: solubility prediction in organic solvents and water,” *Nature Communications*, vol. 11, no. 1, p. 5753, 2020.

[34] J. S. Delaney, “ESOL: Estimating aqueous solubility directly from molecular structure,” *Journal of Chemical Information and Computer Sciences*, vol. 44, no. 3, pp. 1000–1005, 2004.

[35] R.-R. Griffiths, L. Klarner, H. Moss, A. Ravuri, S. Truong, Y. Du, S. Stanton, G. Tom, B. Rankovic, A. Jamasb *et al.*, “GAUCHE: A library for Gaussian processes in chemistry,” *Advances in Neural Information Processing Systems*, vol. 36, 2024.

[36] Z.-M. Win, A. M. Cheong, and W. S. Hopkins, “Using machine learning to predict partition coefficient (Log P) and distribution coefficient (Log D) with molecular descriptors and liquid chromatography retention time,” *Journal of Chemical Information and Modeling*, vol. 63, no. 7, pp. 1906–1913, 2023.

[37] D. Eriksson and M. Jankowiak, “High-dimensional Bayesian optimization with sparse axis-aligned subspaces,” in *Uncertainty in Artificial Intelligence*. PMLR, 2021, pp. 493–503.

[38] G. Brockman, V. Cheung, L. Pettersson, J. Schneider, J. Schulman, J. Tang, and W. Zaremba, “Openai gym,” *arXiv preprint arXiv:1606.01540*, 2016.

[39] D. R. Jones, M. Schonlau, and W. J. Welch, “Efficient global optimization of expensive black-box functions,” *Journal of Global Optimization*, vol. 13, pp. 455–492, 1998.

[40] D. Li, A. Yadav, H. Zhou, K. Roy, P. Thanasekaran, and C. Lee, “Advances and applications of metal-organic frameworks (mofs) in emerging technologies: A comprehensive review,” *Global Challenges*, vol. 8, no. 2, p. 2300244, 2024.

[41] P. D. Leeson, A. P. Bento, A. Gaulton, A. Hersey, E. J. Manners, C. J. Radoux, and A. R. Leach, “Target-based evaluation of “drug-like” properties and ligand efficiencies,” *Journal of medicinal chemistry*, vol. 64, no. 11, pp. 7210–7230, 2021.

[42] R. G  mez-Bombarelli, J. N. Wei, D. Duvenaud, J. M. Hern  ndez-Lobato, B. S  nchez-Lengeling, D. Sheberla, J. Aguilera-Iparraguirre, T. D. Hirzel, R. P. Adams, and A. Aspuru-Guzik, “Automatic chemical design using a data-driven continuous representation of molecules,” *ACS central science*, vol. 4, no. 2, pp. 268–276, 2018.

[43] B. Wang, J. Cai, C. Liu, J. Yang, and X. Ding, “Harnessing a novel machine-learning-assisted evolutionary algorithm to co-optimize three characteristics of an electrospun oil sorbent,” *ACS Applied Materials & Interfaces*, vol. 12, no. 38, pp. 42 842–42 849, 2020.

[44] S. Doncieux, A. Laflaqui  re, and A. Coninx, “Novelty search: A theoretical perspective,” in *Proceedings of the 2019 Genetic and Evolutionary Computation Conference*, 2019, pp. 99–106.